Phonons in GaP quantum dots

Huaxiang Fu, V. Ozoliņš, and Alex Zunger
National Renewable Energy Laboratory, Golden, Colorado 80401
(Received 10 August 1998)

The phonon structure of GaP quantum dots is studied using an atomistic potential model. The dot eigenmodes are obtained from a direct diagonalization of the dynamical matrix and classified using an efficient dual-space analysis method. Our calculations provide a theoretical explanantion for several experimental observations. (1) Depending on the spatial localization, the phonon modes of dots are either dot-interior (bulklike) or surfacelike. (2) The frequencies of the dot-interior modes can be qualitatively described by the ''truncated crystal method'' using a single branch and a single wave vector of the bulk-phonon dispersion. In contrast, the surface modes cannot be described by this model. (3) The dot-interior modes have a dominant bulk parentage from a specific part of the Brillouin zone, while the surface modes do not. (4) The frequencies of the bulklike Γ-derived longitudinal optical (LO) and transverse optical (TO) phonon modes are found to decrease with decreasing dot size. This decrease reflects the downward dispersion of the bulk optical-phonon branches away from the Γ point. (5) The surface modes located between the bulk TO- and LO-phonon bands have a significant bulk Γ character, and are thus Raman detectable. (6) The dot-interior modes exhibit only a slight LO/TO mode mixing, while the surfacelike modes show a strong mode mixing. [S0163-1829(99)12203-3]

I. INTRODUCTION

Phonons in zero-dimensional quantum dots are beginning to attract attention[1–17] because of the interesting differences they exhibit relative to the bulk modes[1–12] and because of the implications for carrier dynamics.[13–17] The lack of translational periodicity in dots affects both the phonon states and the electron-phonon interaction. For example, the removal of the translational symmetry relative to the bulk is predicted to cause mixing[11] of the transverse optical (TO) and longitudinal optical (LO) modes, as recently has been observed by Krauss *et al.*[1] in PbS dots. Furthermore, the exciton-phonon interaction in dots can be enhanced so significantly that it results in a frequency renormalization of the LO-phonon mode, which has been observed by Zimin *et al.*[2] in the absorption spectrum and by Itoh *et al.*[3] in the luminescence spectrum of CuCl dots. Although numerous Raman scattering measurements have been carried out in CdS,[4,5] CdSe,[6] CdS_xSe_{1-x},[7,8] CdTe,[9] and GaP (Ref. 10) dots, the conclusions regarding the dependence of the exciton-phonon coupling strength on the quantum-dot size are conflicting: Shiang *et al.*[4] find that the exciton-phonon coupling decreases with decreasing dot size, while Scamarcio *et al.*[8] find that the coupling increases with decreasing size.

Despite numerous experiments, there are only a few theoretical investigations[11,14–17] of phonons in quantum dots. Since the electronic[18,19] or vibrational states of a *dot* can be thought of as a linear combination of the *bulk* periodic states from different bands and Brillouin-zone wave vectors, it is important that a theory of phonons in dots uses a realistic description of the bulk-phonon dispersion. Indeed, the details of the shift of the vibrational frequencies with the dot size may depend crucially on the bulk-phonon dispersion (see Sec. III D). Almost all of the theories of phonons in dots either neglect the bulk phonon dispersion or assume a continuum model as an approximation (i.e., an elastic model for the acoustic modes[14] and a dielectric model for the optical modes[15–17]). Furthermore, an accurate description of the phonon structure has also been found[12] to be important in calculating the exciton-phonon interactions: the microscopic model and the macroscopic dielectric model for the optical phonons gave[12] rather different scattering rates in GaAs/AlAs quantum wells. The necessity to obtain accurate bulk phonon dispersion curves suggests that an *atomistic* description for phonons in dots is needed. However, the atomistic approach raises another problem, namely, how to analyze and classify the vibrational modes in dot systems consisting of several thousands of atoms. This problem does not occur in simplified model calculations[11,14–17] where the symmetry of the model usually provides series of good quantum numbers to identify the modes.

In the present paper we use an atomistic approach to study the vibrational structure of GaP quantum dots. We develop an empirical valence-force field (VFF), consisting of a short-ranged part to describe the covalent bonding and a long-range part to describe the Coulomb interaction between point-charged ions. This atomistic force field reproduces accurately the bulk-phonon dispersion curves. We apply it to spherical GaP dots containing up to 2000 atoms and use a dual-space method to efficiently analyze and classify several thousands of vibrational modes of these dots. Specifically, we use a ''mode projection approach'' in *reciprocal space* to understand the relationship between the phonons in dots and their counterparts in bulk, while a ''localization radius'' constructed in real space is used to investigate the spatial localization of the dot eigenmodes. Using these techniques, we find that the phonon modes in dots are either bulklike or surfacelike states.

(a) The modes that are localized within the interior of the dot have a clear bulk parentage in terms of their projection onto the bulk-phonon states, and, therefore, can be approximated by a single band at a single-wave vector of the bulk-phonon dispersion. The frequencies of the Γ-derived LO and TO dot-interior modes are found to decrease with decreasing

dot size. This is consistent with experiments.[10] Unlike the case in PbS dots,[1] we find no significant LO/TO mixing for the bulklike modes in GaP dots.

(b) The surfacelike modes are localized at the perifery of the dot, and their eigenvectors are superpositions of many bulk-phonon states from different bands and different points of the Brillouin zone. The surfacelike modes located between the bulk LO- and TO-phonon bands have a significant bulk-Γ character and, thus, may be Raman active. In contrast to the bulklike modes, these surfacelike modes exhibit significant LO/TO mixing.

II. THEORETICAL METHODS

A. Phonon frequencies and eigenstates: Bulk and dots

The atom-atom force field $U(\{\mathbf{r}_i\})=U_{\rm SR}+U_{\rm LR}$ used here includes a short-range part $U_{\rm SR}$, which describes the covalent bonding, and a long-range part $U_{\rm LR}$, which describes the Coulomb interaction between point-charged ions. For atom i bonded tetrahedrally to atoms j and k, the short-range interaction is

$$\begin{aligned}U_{\rm SR}(\{\mathbf{r}_i\})=&\frac{1}{a_0^2}\sum_{i<j}\alpha_{ij}(\mathbf{r}_{ij}^2-a_0^2)^2\\&+\frac{1}{a_0^2}\sum_i\sum_{j<k}\beta_{jik}(\mathbf{r}_{ij}\cdot\mathbf{r}_{ik}-\mathbf{r}_{ij}^0\cdot\mathbf{r}_{ik}^0)^2\\&+\frac{1}{a_0^2}\sum_i\sum_{j<k}\gamma_{jik}(\mathbf{r}_{ij}^2-a_0^2)(\mathbf{r}_{ij}\cdot\mathbf{r}_{ik}-\mathbf{r}_{ij}^0\cdot\mathbf{r}_{ik}^0)\\&+\frac{1}{a_0^2}\sum_i\sum_{j<k}\delta_{jik}(\mathbf{r}_{ij}^2-a_0^2)(\mathbf{r}_{ik}^2-a_0^2),\end{aligned}\tag{1}$$

where $\mathbf{r}_{ij}=\mathbf{r}_i-\mathbf{r}_j$ is the vector connecting atoms i and j, and $\{\alpha_{ij},\beta_{jik},\gamma_{jik},\delta_{jik}\}$ are short-range force constants. a_0 is the equilibrium bond length. The first two terms in Eq. (1) are the bond-stretching and bond-bending terms familiar from the commonly used Keating's VFF models,[20–23] while the remaining two terms describe the coupling between the bond-stretching and bond-bending and between the bond-stretchings of two nearest bonds, respectively. For compound semiconductors there is an additional Coulomb interaction[21,22] term between the ions, which is simulated by point charges at the ionic positions:

$$U_{\rm LR}(\{\mathbf{r}_i\})=\sum_{i<j}\frac{Z_i^*Z_j^*}{\epsilon(\infty)|\mathbf{r}_i-\mathbf{r}_j|}.\tag{2}$$

Here, Z_i^* is the effective charge of ion i, and $\epsilon(\infty)$ is the dielectric constant at infinite frequency. We use Ewald's method[24] to calculate the sum in Eq. (2) for periodic-bulk systems. For finite quantum dots, the summation in Eq. (2) is calculated directly.

The atomic force constants $\Phi_{\rho,\sigma}(i,j)$ are obtained from the force field $U=U_{\rm SR}+U_{\rm LR}$ as

$$\Phi_{\rho,\sigma}(i,j)=\frac{\partial^2U}{\partial r_{i\rho}\partial r_{j\sigma}},\tag{3}$$

TABLE I. The force-field parameters (in units of N/m) and the effective charges used in the present calculation. The dielectric constant is $\epsilon(\infty)=9.11$.

atom i	α_{ij}	β_{jik}	γ_{jik}	δ_{jik}	Z^*
Ga	96.07	−31.75	−11.75	19.66	2.05
P	96.07	57.07	29.57	19.66	−2.05

where ρ and σ label the Cartesian coordinates. The phonon frequencies $\omega_{n\mathbf{k}}\equiv 2\pi\nu_{n\mathbf{k}}$ (of branch n and wave vector $\mathbf{k}$) and eigenmodes $\mathbf{Q}_{n\mathbf{k}}(\xi)$ of bulk GaP are then obtained by diagonalizing the dynamical matrix:

$$\sum_{\sigma,\xi'}[D_{\rho,\sigma}(\xi\xi'|\mathbf{k})-\omega_{n\mathbf{k}}^2\delta_{\rho\sigma}\delta_{\xi\xi'}]Q_{n\mathbf{k}}^{\sigma}(\xi')=0.\tag{4}$$

Here ξ is the atomic index inside the primary cell, i.e., $\mathbf{r}_i=\mathbf{r}_\xi+\mathbf{R}_l$, where $\mathbf{R}_l$ is a lattice vector. The matrix element $D_{\rho,\sigma}(\xi\xi'|\mathbf{k})$ is

$$D_{\rho,\sigma}(\xi\xi'|\mathbf{k})=\frac{1}{\sqrt{M_\xi M_{\xi'}}}\sum_{l'}\Phi_{\rho,\sigma}(l\xi,l'\xi')e^{-i\mathbf{k}\cdot[\mathbf{R}(l)-\mathbf{R}(l')]},\tag{5}$$

where M is the mass of atom. The displacement of atom i corresponding to the phonon eigenmode $\mathbf{Q}_{n\mathbf{k}}(\xi)$ is

$$\mathbf{u}_{n\mathbf{k}}(i)=\frac{1}{\sqrt{M_\xi}}\mathbf{Q}_{n\mathbf{k}}(i)e^{i\mathbf{k}\cdot\mathbf{R}_l}.\tag{6}$$

Equations (1)–(6) are also valid for quantum dots except that only $\mathbf{k}=0$ is considered.

The constants $\{\alpha_{ij},\beta_{jik},\gamma_{jik},\delta_{jik}\}$ of the short-range force field in Eq. (1) and the ion-effective charge Z_i^* in Eq. (2) are obtained by fitting the calculated bulk-phonon frequencies of GaP to the experiment.[26,27] Specifically, the effective charge is calculated from the experimental LO/TO splitting at the zone center Γ point using the relation[28]

$$\omega_{\rm LO}^2=\omega_{\rm TO}^2+4\pi\frac{1}{\Omega}\frac{(Z_i^*)^2}{\mu\epsilon(\infty)},\tag{7}$$

where Ω is the volume of the bulk-unit cell, and μ is the reduced mass of the two atoms in the compound semiconductor. The short-range interatomic interaction parameters are then obtained by fitting the measured[26,27] phonon frequencies at bulk Γ, X, and L points using a least-square procedure. The resulting parameters for GaP are given in Table I.

B. Method for analyzing the dot eigenmodes

For quantum dots with several thousands of phonon eigenmodes it is important to find an efficient and transparent way of analyzing the characters of these numerous eigenmodes. We do this by using a dual-space technique (i.e., in real space and in reciprocal space).

In real space, we define the ''localization radius'' for a normal mode λ as

$$R_\lambda^2 = \sum_i \sum_{\rho=1}^{3} |Q_\lambda^\rho(i)|^2 |\mathbf{r}_i - \mathbf{r}_c|^2, \tag{8}$$

where $\mathbf{r}_c$ is the dot center. R_λ tells us in what part of the dot is the eigenmode λ localized, distinguishing modes that are localized inside the dot (''bulklike modes'') from those localized at the periphery of the dot (''surfacelike modes'').

In reciprocal space we use the projection approach to establish the relation between the dot modes and the bulk modes.[25] We first expand the dot displacements $\mathbf{u}_\lambda^{\rm dot}$ in the bulk states $\mathbf{u}_{n\mathbf{k}}^{\rm bulk}$ of branch n and wave vector $\mathbf{k}$:

$$\mathbf{u}_\lambda^{\rm dot}(i) = \sum_n \int d\mathbf{k} C_{n\mathbf{k}}^{(\lambda)} \mathbf{u}_{n\mathbf{k}}^{\rm bulk}(i). \tag{9}$$

The projection coefficients $C_{n\mathbf{k}}^{(\lambda)}$ are calculated using the orthogonality of $\mathbf{u}_{n\mathbf{k}}^{\rm bulk}$. We define the *Brillouin-zone parentage* $P_\lambda(k)$ of a dot mode λ as the contribution of the bulk eigenmodes with the wavevector length k in forming this dot mode:

$$P_\lambda(k) = \int d\mathbf{k} \delta(|\mathbf{k}| - k) \sum_n |C_{n\mathbf{k}}^{(\lambda)}|^2. \tag{10}$$

This quantity tells us which part of the bulk Brillouin zone (BZ) contributes to a given dot eigenmode. We also define the *bulk*-Γ *parentage* $T_\lambda(n, K_{\rm cut})$ measuring the extent to which the dot eigenmode is derived from the bulk states near Γ:

$$T_\lambda(n, K_{\rm cut}) = \int_0^{K_{\rm cut}} dk \int d\hat{\mathbf{k}} |C_{n\mathbf{k}}^{(\lambda)}|^2, \tag{11}$$

where $\hat{\mathbf{k}}$ is the direction angle of wave vector $\mathbf{k}$. Typically, we choose $K_{\rm cut}$ as $2\sqrt{3}\pi/D$ (where D is the diameter of the dot), which is determined by the first node $k = 2\pi/D$ of the spherical Bessel function $j_0(kr)$. Finally, in order to investigate the possibility of mode mixing in dots, we define the *bulk-band parentage* of the dot mode λ as

$$A_\lambda(n) = \int d\mathbf{k} |C_{n\mathbf{k}}^{(\lambda)}|^2. \tag{12}$$

When $A_\lambda(n)$ of the dot mode λ has significant contributions from different *bulk* phonon bands n, we say that there is a ''mode mixing,'' e.g., LO with TO.

III. RESULTS AND DISCUSSIONS

A. Phonon dispersion of bulk GaP

Figure 1 shows the calculated phonon-dispersion curves of bulk GaP, compared with the experimental data.[26,27] The calculated TO- and LO-phonon frequencies ν at Γ are 10.97 and 11.98 THz, respectively, close to the experimental values[27] of 10.95 and 12.06 THz. Although the theoretical fit is done only at the Γ, X, and L points, Fig. 1 shows that the calculated dispersion curves agree well with the experimental data throughout the Brillouin zone for both the acoustic and optical branches. Specifically, the downward dispersion of the bulk TO- and LO-phonon bands near the Γ point is reproduced quite well by our model. We will see later (Sec. III D) that this feature is important for describing the size

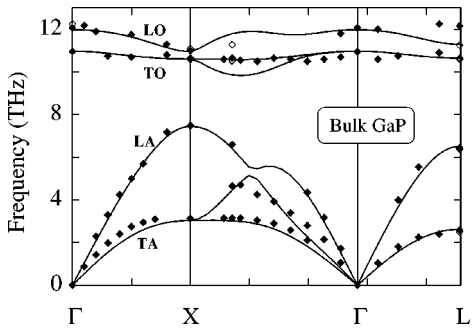

FIG. 1. The calculated phonon dispersion of bulk GaP (solid lines), in comparison with experimental data (Refs. 26 and 27) (symbols).

dependence of phonon frequencies in quantum dots. The calculated bulk dispersion also agrees well with the recent first-principles result obtained by Ozoliņš and Zunger[29] using the density-functional linear-response theory. For example, the largest frequency difference between the LO- and TO-phonon bands along the [111] direction is 2.04 THz in our model and 1.70 THz in the first-principles calculation.[29] In comparison, an earlier calculation of Kushwaha and Kushwaha[30] using an eight-parameter bond-bending force model gave 3.8 THz as the largest LO/TO frequency difference, and the calculation of Kagaya and Soma[31] using the Heine-Abarenkov model potential gave an upward TO band dispersion.

B. Phonons in GaP quantum dots

We have studied four spherical GaP dots: $Ga_{140}P_{141}$, $Ga_{240}P_{225}$, $Ga_{456}P_{435}$, and $Ga_{1060}P_{1061}$ with diameters D=22.2, 26.2, 32.5, and 43.4 Å, respectively. The atomic positions in the dots are assumed to be the same as in the bulk. We use the same force field for GaP dots as that used for the bulk, except that the boundary condition is changed appropriately. We aim to simulate ''free-standing'' quantum dots such as those generated in porous form by anodization current.[10] The dot surface is thus assumed to be free without passivating atoms and without surface reconstruction. We directly diagonalize the full dynamical matrix of Eq. (5) to obtain the phonon frequencies and eigenmodes, which are then subjected to the analysis of Eqs. (10)–(12).

Figure 2(a) shows the phonon densities of states (DOS) for the four studied dots. The phonon DOS has been broadened by a Gaussian with a width of 0.9 THz. We also show, for comparison, the bulk-phonon DOS, calculated using 408 special $\mathbf{k}$ points[32] in the irreducible Brillouin zone (corresponding to 4096 $\mathbf{k}$ points in the whole zone). Note that in the following we use ν^2 rather than ν as the x-axis scale in order to achieve higher resolution in the optical region. Due to the absence of passivation at the dot surface, a few dot modes ($\sim$10 out of several thousands, not shown in Fig. 2) are found to have very small imaginary frequencies, signaling a dynamical instability of the unpassivated dots. We note from Fig. 2(a) the following features.

(i) While the phonon DOS of the small dot (D = 22.2 Å) is quite different from the bulk DOS, they become more similar with increasing dot size.

(ii) Some phonon modes appear in the frequency range where there are no bulk modes. These regions are shaded in

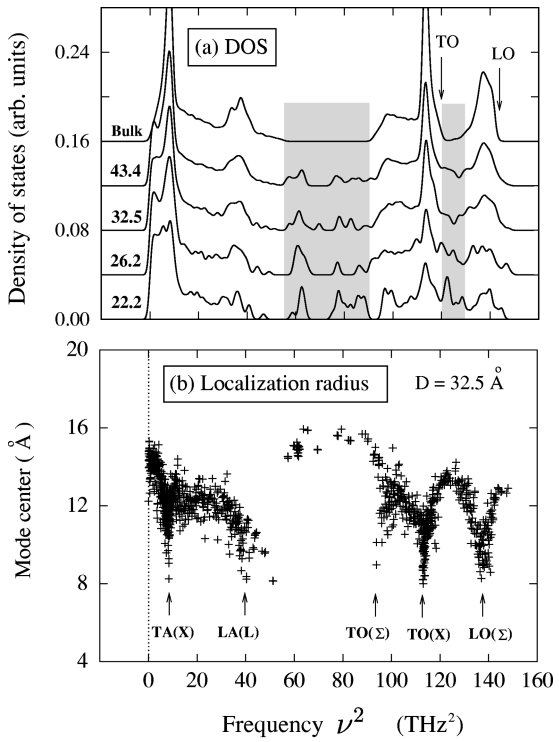

FIG. 2. (a) Density of phonon states for GaP quantum dots of different sizes. The diameters of dots (in Å) are indicated on the left side of each curve. The bulk phonon DOS is also shown for comparison. The shaded areas mark the frequency regions where surfacelike dot modes appear. The bulk TO- and LO-phonon frequencies are indicated by vertical arrows. (b) *Localization radii* [Eq. (8)] of the $D=32.5$ Å dot, measuring the location of the mode with respect to the center of the dot. The identities [e.g., TA(X)] of highly localized modes (with small localization radii) are indicated by vertical arrows.

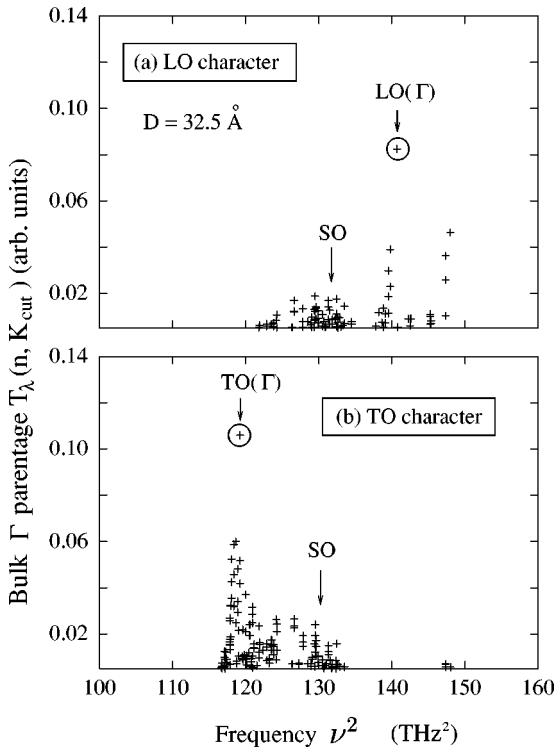

FIG. 3. ''Bulk Γ parentage'' $T_\lambda(n,K_{\rm cut})$ [Eq. (11)] of the phonon modes of the $D=32.5$ Å dot for bulk-phonon branch n. Part (a) shows the contribution from bulk LO ($n=6$) phonons and part (b) shows the contribution from bulk TO ($n=4+5$) phonons. We use $K_{\rm cut}=2\sqrt{3}\pi/D$ in Eq. (11). The ''localization radii'' for this dot are shown in Fig. 2(b).

Fig. 2. Region I ($\nu^2=60$–90 THz^2) is the phonon gap between the bulk acoustic and optical modes, and region II ($\nu^2=120$–130 THz^2) is the phonon gap between the bulk TO and LO modes. We will see later from the ''localization radii'' [Fig. 2(b)] that these ''gap modes'' are localized on the dot surface.

(iii) Although the ''gap modes'' exist even in the very large dots (with several thousands of atoms), their peak intensities relative to the bulklike modes decrease significantly with increasing dot size.

C. Mode analysis using the dual-space approach

The ''localization radii'' [see Eq. (8)] for the dot with diameter $D=32.5$ Å are shown in Fig. 2(b). Comparison with the phonon DOS in Fig. 2(a) shows the following features.

(i) The gap modes in regions I and II have their mode centers close to the dot's surface [Fig. 2(b)], thus being ''surfacelike modes.''

(ii) The dot modes that correspond to the sharp peaks of the bulk DOS have their localization radii in the dot's interior, thus being ''bulklike'' (dot-interior) modes. Our ''Brillouin-zone parentage'' analysis and the frequencies of the dot modes indicate that the modes at $\nu^2=9$, 40, 95, 113, and 138 THz^2 in Fig. 2(b) are derived from the bulk TA(X) (TA modes near the X point), LA(L), TO(Σ) (TO modes along the [110] direction), TO(X), and LO(Σ) modes, respectively. These dot-interior modes are clearly separated from the surface modes.

(iii) The dot modes with intermediate localization radii (around 11 Å in Fig. 2) have their vibrational amplitudes both inside the dots and near the dot surface.

(iv) We find that the distributions of localization radii R_λ vs ν_λ for different dot sizes contain similar features [compare Fig. 2(b) with Fig. 6 below, showing the localization radii of a much smaller dot]. This surprising ''self-similarity'' exists for both the dot-interior modes and the surfacelike modes, and it holds to the smallest dot size considered.

To study the evolution of an individual dot mode with the size D, we have to identify the same phonon mode in different dots. We are particularly interested in the dot modes that derive from the bulk Γ states, since such modes play an important role in Raman scattering. We use for this purpose the ''bulk-Γ parentage'' $T_\lambda(n,K_{\rm cut})$ defined in Eq. (11). Figure 3(a) shows the bulk-Γ LO character and Fig. 3(b) gives the bulk-Γ TO character for the $D=32.5$ Å dot phonons with frequencies above 10 THz. We see in Fig. 3(a) that a single dot mode [labeled LO(Γ)] originates predominantly from the bulk LO phonon near Γ, and another dot mode [labeled TO(Γ)] originates predominantly from the bulk-TO phonon near Γ. Between these TO(Γ)- and LO(Γ)-like modes there exist some surface modes [denoted as spin orbit (SO) in Fig. 3, see Fig. 2(b) for their localization radii], which have con-

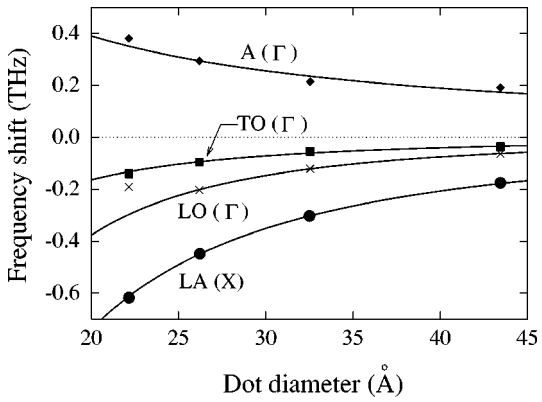

FIG. 4. Variation of the frequencies of the $A(\Gamma)$, LA(X), TO(Γ), and LO(Γ) dot modes with the dot size. The corresponding bulk frequencies are taken as zero reference points.

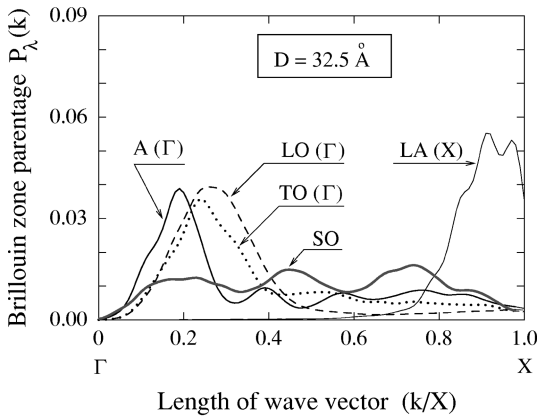

FIG. 5. ''Brillouin-zone parentages'' $P_\lambda(k)$ [Eq. (10)] of the bulklike $A(\Gamma)$, LA(X), TO(Γ), LO(Γ), and surfacelike SO modes of the $D=32.5$ Å dot. The definition of these modes is given in Sec. III D.

tributions from both bulk TO- and LO-phonon bands. The fact that the surface modes in Fig. 3 have sizable contributions from bulk **k** points near Γ implies that these modes might be Raman active. Indeed, in a micro-Raman scattering study of porous GaP nanocrystallites, Tiginyanu *et al.*[10] observed a small peak between sharp bulk derived LO- and TO-phonon peaks. They suggested that the origin of this peak is due to the dot surface—a suggestion that is supported by our theoretical result.

D. Evolution of mode frequencies with dot size

Once the character of the dot modes is identified for different dot sizes (Fig. 3), we can trace the size dependence of the frequencies of these modes (Fig. 4). In order to facilitate the understanding of the evolution of phonon frequency with the dot size, we choose four special modes: the bulk-derived LO(Γ) and TO(Γ), the Γ-derived acoustic mode $A(\Gamma)$, which is the dot's mode of the lowest-acoustic frequency, and the X-derived longitudinal acoustic mode LA(X), which is the dot's mode of the highest-acoustic frequency. The Γ character of the $A(\Gamma)$ mode and the X character of the LA(X) mode can be seen from their Brillouin-zone parentages (see Fig. 5 below). These four modes are all dot-interior states according to their localization radii. We see from Fig. 4 that both the TO(Γ) and LO(Γ) modes shift *down* in frequency with decreasing dot size. This is consistent with the experimental measurements[10] where both LO- and TO-phonon Raman peaks were found to shift to lower frequencies with inceasing anodization current (i.e., decreasing dot size) in porous GaP nanocrystallites. The frequency of the acoustic mode $A(\Gamma)$ *increases* as the dot size decreases.

Analytically fitting the calculated results gives

$$\Delta\nu=\begin{cases} 8.84/D^{1.04} & [A(\Gamma)] \\ -74.75/D^{2.04} & [\mathrm{TO}(\Gamma)] \\ -392.77/D^{2.32} & [\mathrm{LO}(\Gamma)] \\ -181.52/D^{1.84} & [\mathrm{LA}(X)], \end{cases} \tag{13}$$

where $\Delta\nu$ is in units of THz and D is in units of Å. The fitted results are shown in Fig. 4 as solid lines. We see that, while the frequency shift of the $A(\Gamma)$ mode is almost inversely linear with the dot size, it is close to $1/D^2$ for the other three modes.

To understand this frequency shift with the dot size, we recall from Eq. (9) that, in general, the frequency of a *bulk-like* mode can be expressed as a linear combination of the bulk-phonon frequencies:

$$(\nu_\lambda^{\mathrm{dot}})^2 \cong \sum_{n,\mathbf{k}} |C_{n\mathbf{k}}^{(\lambda)}|^2 (\nu_{n\mathbf{k}}^{\mathrm{bulk}})^2. \tag{14}$$

One may wonder whether, given $\{\nu_{n\mathbf{k}}^{\mathrm{bulk}}\}$, there is a way to guess $\nu_\lambda^{\mathrm{dot}}$ without doing a full calculation of $C_{n\mathbf{k}}^{(\lambda)}$. Specifically, the question is whether there exists in Eq. (14) a single wave vector $\mathbf{k}^*$ and a single branch n, most associated with the dot mode λ, which satisfies

TABLE II. Comparison of the frequencies of the four dot modes $A(\Gamma)$, LA(X), TO(Γ), and LO(Γ), described by Eq. (13), as obtained from direct diagonalization of the dot's dynamical matrix and as obtained from the truncated crystal method of Eq. (15) (in parentheses). Isotropically averaged bulk-phonon dispersion is used in the truncated-crystal model for spherical dots.

	Frequencies of dot modes (THz)			
Dot diameter (Å)	$A(\Gamma)$	LA(X)	TO(Γ)	LO(Γ)
22.2	0.38 (1.19)	6.84 (6.20)	10.83 (10.91)	11.79 (11.90)
26.2	0.29 (1.02)	7.01 (6.29)	10.88 (10.93)	11.78 (11.92)
32.5	0.21 (0.83)	7.15 (6.35)	10.92 (10.94)	11.86 (11.94)
43.4	0.19 (0.62)	7.28 (6.38)	10.94 (10.95)	11.92 (11.96)

TABLE III. Bulk-band parentage $A_\lambda(n)$ [Eq. (12)] of bulk-phonon bands ($n=1,\ldots,6$) in forming the $A(\Gamma)$, LA(X), TO(Γ), LO(Γ), and SO modes of the $D=32.5$ Å dot.

	Contribution $A_\lambda(n)$ (in %) of bulk band n to dot mode λ			
Dot mode λ	$n=1+2$ (TA)	$n=3$ (LA)	$n=4+5$ (TO)	$n=6$ (LO)
$A(\Gamma)$	**86.5**	3.9	8.1	1.5
LA(X)	0.8	**91.3**	4.1	3.9
TO(Γ)	5.4	0.5	**87.7**	6.4
LO(Γ)	0.1	3.6	0.9	**95.4**
SO	1.9	4.1	**31.5**	**62.5**

$$\nu_\lambda^{\rm dot}\approx\nu_{n\mathbf{k}^*}^{\rm bulk}. \tag{15}$$

We use the ''Brillouin-zone parentage'' $P_\lambda(k)$ to answer this. Figure 5 shows, for the $D=32.5$ Å dot, the Brillouin-zone parentages of the bulklike $A(\Gamma)$, TO(Γ), LO(Γ), and LA(X) modes with frequencies $\nu^2=0.046$, 119.2, 140.7, and 51.1 THz^2, respectively.

We see from Fig. 5 that the above considered bulklike modes all have a dominant BZ parentage peak around their bulk origins [e.g., $A(\Gamma)$, TO(Γ), LO(Γ) near Γ, and LA(X) near X], i.e., for the bulklike dot modes there exists a $\mathbf{k}^*$ that satisfies Eq. (15). For the Γ-derived $A(\Gamma)$, TO(Γ), and LO(Γ) modes, the peak positions of the Brillouin-zone parentages are located near $|\mathbf{k}^*|=2\pi/D$. In fact, this $\mathbf{k}^*$ has been used[33] in the ''truncated crystal'' method to estimate the electronic-orbital energy in dots from the bulk-band structure using Eq. (15). In the truncated-crystal method one seeks a wave vector $\mathbf{k}^*$ for which the envelope function vanishes at the dot boundary. For spherical dots the smallest k^* that satisfies this boundary condition is $2\pi/D$. This approach then relates the *bulk dispersion* $\nu_{n\mathbf{k}}$ to the frequency ν_λ in dots. The smaller the dot, the further does $k^*\propto 1/D$ move away from the Γ point. Thus, the slope of the bulk dispersion away from Γ determines, in this model, the size dependence of the frequency of the dot's mode. Since the frequency of the bulk GaP optical phonons (Fig. 1) decreases when $\mathbf{k}$ departs from the Γ point, the frequencies of the dot's TO(Γ) and LO(Γ) modes should exhibit a *redshift* relative to their bulk values. This expectation is confirmed by our results obtained from the direct diagonalization of the dynamical matrix (Fig. 4). The scaling exponent τ of $1/D^\tau$ in Eq. (13) can also be qualitatively understood from a TC-type argument: since the frequencies of the bulk acoustic-phonon branches near Γ are linear functions of the wave vector $\nu\propto k$, and since $k^*\propto 1/D$, we obtain that $\delta\nu\propto 1/D$ (i.e., $\tau=1$), as indeed given by Eq. (13) for the $A(\Gamma)$ mode. The bulk-phonon dispersion relations of the LO- and TO-phonon modes at Γ and of the LA-phonon mode at X are parabolic and, thus, lead to $\delta\nu\propto 1/D^2$, i.e., $\tau\approx 2$ in Eq. (13). More quantitatively, Table II compares the frequencies of the bulklike dot modes, as obtained from direct calculations, with those obtained from Eq. (15). We see that the two methods give the same trend of the frequency change with the dot size, and that they give quantitatively accurate results for the bulklike LO- and TO-derived modes. However, for the $A(\Gamma)$ dot-phonon mode, the frequencies obtained from the two methods are quite different. This is probably due to the surface effect, which causes this mode to have a large localization radius [e.g., $R_\lambda\approx 12$ Å in Fig. 2(b)] and, therefore, destroys the conditions for the applicability of the truncated-crystal model.

Since the surfacelike modes are localized in real space on the dot surface and, therefore, contain contributions from the bulk GaP modes all over the Brillouin zone, there is not a single $\mathbf{k}^*$ to be used in Eq. (15) to describe their frequencies. This property of the surface modes is illustrated in Fig. 5, which shows, for comparison with the bulklike $A(\Gamma)$, LO(Γ), TO(Γ), and LA(X) modes, the Brillouin-zone parentage of a surfacelike optical (SO) mode with $\nu^2=126.6$ THz^2 for the $D=32.5$ Å dot. We see from Fig. 5 that the surfacelike mode is delocalized in reciprocal space.

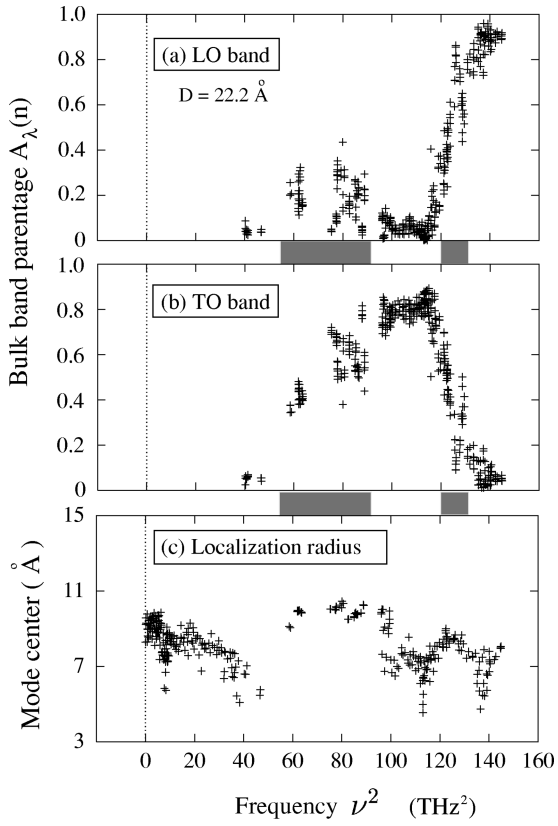

FIG. 6. ''Bulk-band parentage'' $A_\lambda(n)$ [Eq. (12)] of (a) $n=6$ (bulk LO-phonon band) and (b) $n=4+5$ (bulk TO-phonon bands) in forming dot modes with frequency $\nu^2>40$ THz^2. The results for the $D=22.2$ Å dot are shown. The shaded areas indicate the modes that have a sizable LO/TO mode mixing. Panel (c) shows the localization radii of the dot modes in order to facilitate the comparison.

E. Mode mixing

An interesting possibility is the LO/TO mode mixing of the phonon modes in quantum dots, which can be induced by the lack of translational symmetry in dots. Table III gives the ''bulk-band parentage'' [Eq. (12)] of the five dot modes shown in Fig. 5 for the $D=32.5$ Å quantum dot. We see that in this relatively large dot there is no significant mode mixing for the bulk-derived $A(\Gamma)$, TO(Γ), LO(Γ), and LA(X) modes. However, there exists a significant LO/TO mode mixing for the surface-related SO mode. This effect persists even in the very small GaP dots; Fig. 6(a) shows the bulk TO and LO band parentage [Eq. (12)] for the modes of the $D=22.2$ Å dot. Again, we see that significant LO/TO mode mixing exists only in the frequency range where, according to the analysis of the localization radii in Fig. 6(c), the modes are surfacelike.

IV. SUMMARY

We have developed an atomic-force field for GaP, which gives an accurate bulk-phonon dispersion. This atomistic model is then used to calculate the phonon frequencies and eigenmodes of GaP quantum dots. The resulting several thousands of dot eigenmodes have been analyzed using the projection approach in reciprocal space and the localization radius in real space. We have found that the surface modes can be distinguished from the bulklike modes in both reciprocal and real space. In particular, we conclude the following.

(1) The *bulklike modes* are localized inside the dot and have a clearly pronounced bulk Brillouin-zone parentage in reciprocal space. The frequencies of these modes can be approximated by the ''truncated crystal method'' with a single-bulk phonon band at a single-wave vector $\mathbf{k}^*$. The bulklike Γ-derived TO- and LO-phonon dot modes both shift down in frequency with decreasing dot size. Unlike the case in PbS dots,[1] there is almost no LO/TO mixing for the bulklike modes.

(2) The *surface modes* are located in the frequency range $\nu^2=120-130$ THz^2 between the bulk TO- and LO-phonon bands, and in the range $\nu^2=60-90$ THz^2 between the bulk LA- and TO-phonon bands. These surface modes are localized at the perifery of the dot. Their eigenmodes represent a superposition of many bulk bands with $\mathbf{k}$ points from all over the bulk Brillouin zone. The surface dot modes in the frequency range $\nu^2=120-130$ THz^2 have considerable bulk TO and LO characters and, therefore, should be Raman active. There is significant LO/TO mode mixing for the surfacelike dot modes.

ACKNOWLEDGMENT

This work was supported by the U.S. Department of Energy, OER-BES, under Grant No. DE-AC36-83CH10093.

[1] T. D. Krauss, F. W. Wise, and D. B. Tanner, Phys. Rev. Lett. **76**, 1376 (1996).
[2] L. Zimin, S. V. Nair, and Y. Masumoto, Phys. Rev. Lett. **80**, 3105 (1998).
[3] T. Itoh, M. Nishijima, A. I. Ekimov, C. Gourdon, Al. L. Efros, and M. Rosen, Phys. Rev. Lett. **74**, 1645 (1995).
[4] J. J. Shiang, S. H. Risbud, and A. P. Alivisatos, J. Chem. Phys. **98**, 8432 (1993).
[5] L. Saviot, B. Champagnon, E. Duval, and A. I. Ekimov, Phys. Rev. B **57**, 341 (1998).
[6] C. Trallero-Giner, A. Debernardi, M. Cardona, E. Menendez-Proupin, and A. I. Ekimov, Phys. Rev. B **57**, 4664 (1998).
[7] B. Champagnon, B. Andrianasolo, and E. Duval, J. Chem. Phys. **94**, 5237 (1991).
[8] G. Scamarcio, V. Spagnolo, G. Ventruti, M. Lugara, and G. C. Righini, Phys. Rev. B **53**, R10 489 (1996).
[9] A. M. de Paula, L. C. Barbosa, C. H. B. Cruz, O. L. Alves, J. A. Sanjurjo, and C. L. Cesar, Appl. Phys. Lett. **69**, 357 (1996).
[10] I. M. Tiginyanu, G. Irmer, J. Monecke, and H. L. Hartnagel, Phys. Rev. B **55**, 6739 (1997).
[11] E. Roca, C. Trallero-Giner, and M. Cardona, Phys. Rev. B **49**, 13 704 (1994).
[12] H. Rucker, E. Molinari, and P. Lugli, Phys. Rev. B **44**, 3463 (1991).
[13] V. I. Klimov and D. W. McBranch, Phys. Rev. Lett. **80**, 4028 (1998).
[14] S. Nomura and T. Kobayashi, Solid State Commun. **82**, 335 (1992).
[15] A. V. Fedorov, A. V. Baranov, and K. Inoue, Phys. Rev. B **56**, 7491 (1997).
[16] S. Nomura and T. Kobayashi, Phys. Rev. B **45**, 1305 (1992).
[17] M. C. Klein, F. Hatche, D. Ricard, and C. Flytzanis, Phys. Rev. B **42**, 11 123 (1990).
[18] A. Zunger, MRS Bull. **23**, 35 (1998).
[19] H. Fu, L. W. Wang, and A. Zunger, Phys. Rev. B **57**, 9971 (1998).
[20] P. N. Keating, Phys. Rev. **145**, 637 (1966).
[21] R. M. Martin, Phys. Rev. B **1**, 4005 (1970).
[22] W. Weber, Phys. Rev. B **15**, 4789 (1977).
[23] J. L. Martins and A. Zunger, Phys. Rev. B **30**, 6217 (1984).
[24] A. A. Maradudin, E. W. Montroll, G. H. Weiss, and I. Ipatova, in *Solid State Physics*, edited by H. Ehrenreich, F. Seitz, and D. Turnbull (Academic, New York, 1971), Suppl. 3, p. 200.
[25] H. Fu and A. Zunger, Phys. Rev. B **57**, R15 064 (1998).
[26] P. H. Borcherds, G. F. Alfrey, D. H. Saunderson, and A. D. B. Woods, J. Phys. C **8**, 2022 (1975).
[27] P. Podaar, Phys. Status Solidi B **120**, 207 (1983).
[28] *Solid State Physics*, Ref. 24, p. 254.
[29] V. Ozoliņš and A. Zunger, Phys. Rev. B **57**, R9404 (1998).
[30] M. S. Kushwaha and S. S. Kushwaha, Can. J. Phys. **58**, 351 (1980).
[31] H. M. Kagaya and T. Soma, Phys. Status Solidi B **124**, 37 (1984).
[32] H. J. Monkhorst and J. D. Pack, Phys. Rev. B **13**, 5188 (1976).
[33] A. Zunger, J. Phys. C **7**, 76 (1974); M. V. Rama Krishna and R. A. Friesner, Phys. Rev. Lett. **67**, 629 (1991); S. B. Zhang, C. Y. Yeh, and A. Zunger, Phys. Rev. B **48**, 11 204 (1993); A. Franceschetti and A. Zunger, J. Chem. Phys. **104**, 5572 (1996).